Soft Computing (2019) 23:9899–9917
https://doi.org/10.1007/s00500-018-3544-8

METHODOLOGIES AND APPLICATION

A hybrid teaching–learning-based optimization technique for optimal DG sizing and placement in radial distribution systems

Imran Ahmad Quadri[1] · Suman Bhowmick[1] · Dheeraj Joshi[1]

Published online: 27 September 2018

Abstract

Distributed generation (DG) technology has proved to be an efficient and economical way of generation of power. DGs are intended to generate power near the load centers. Optimal allocation of DG resources enhances the overall performance of distribution systems. This paper presents a hybrid teaching–learning-based optimization (HTLBO) technique for the optimal allocation of DGs in distribution systems. The proposed technique is proficient in handling continuous as well as discrete variables and has the capability to escape strong local minima/maxima trappings. The validity and effectiveness of HTLBO are tested on well-defined standard mathematical benchmark functions. The proposed method is further implemented for optimal allocation of DGs in the IEEE 33-bus, 69-bus and 118-bus radial distribution test systems for minimization of power losses, voltage deviation and maximization of voltage stability index. The multi-objective function for DG allocation uses the ε-constraints approach. The obtained results reveal improved convergence characteristics over both teaching–learning-based optimization and quasi-oppositional teaching–learning-based optimization.

Keywords Distributed generation · Optimization technique · TLBO · QOTLBO · HTLBO

1 Introduction

As compared to centralized bulk power generation, transmission and distribution of power at the load centers constitute major challenges for the utilities. Hence, distributed generation (DG) is a viable option where power is generated near the load centers. DG comprises both fossil fuel-based conventional and nonconventional energy sources like solar power, hydro-, biofuel, geothermal, etc., ranging from few kilowatts to about 50 MW (Singh et al. 2009). Competitive markets, environmental issues and reliability of power sources are some of the major criteria for the selection of energy sources. Depletion of fossil fuel sources and continuous improvement in the area of nonconventional ones have been the motivating factors for the utilities to go for DG.

Proper siting and sizing of DGs is crucial for better distribution system performance. Optimal sizing and placement of DGs play a crucial role in the reduction of power losses, line loading and system operating costs along with improvement in system reliability and prevention of voltage collapse. Earlier, for the voltage profile improvement in power systems, capacitor banks and synchronous condensers were predominantly used (Nagrath and Kothari 2007). But nowadays, to improve the performance of power systems, both active and reactive power injections are carried out using DGs. Therefore, finding the optimal location and size of DGs has been a global challenge for both the academia and the industry.

Several comprehensive research works have been reported in the area of optimal allocation of DGs to improve distribution system performance. A noniterative analytical method for single DG placement in both radial and meshed systems has been presented in Wang and Nehrir (2004) to minimize system power losses for both time-variant- and -invariant-type loads in the IEEE 6-bus and IEEE 30-bus distribution systems. A very efficient analytical method employing BIBC approach for siting and sizing of DGs in the IEEE 12-bus, 34-bus and 69-bus system has been proposed in Gözel and Hocaoglu (2009). However, Gözel and Hocaoglu (2009) is limited to placement of a single DG. An analytical method for multiple DG placements based on the active and reactive components of the branch currents has been reported in Gopiya Naik et al. (2015). Hung et al. (2010) have pre-

Communicated by V. Loia.

✉ Imran Ahmad Quadri
imranquadri83@gmail.com

[1] Electrical Engineering Department, Delhi Technological University, Delhi, India

sented an improved analytical (IA) method for single DG placement and has highlighted its superiority over existing methods based on the assumption that the DG power factor is same as the aggregate load power factor. This method reduces the computational time significantly while considering various types of DGs to minimize power losses and improve the voltage profile of the network. Although analytical methods for siting and sizing of DGs have fast convergence, with increase in the types and number of DGs, the computational complexity increases and may lead to nonoptimal solutions.

Advances in soft computing techniques have led to the development of several optimization algorithms for optimal allocation of DGs. In this perspective, Singh et al. (2008), Ameli et al. (2014), Gomez-Gonzalez et al. (2012), Moradi and Abedini (2012), Niknam et al. (2011), Saha and Mukherjee (2016), Abu-Mouti and El-Hawary (2011), Sheng et al. (2016), Mohanty and Tripathy (2016) and Martín García and Gil Mena (2013) have presented some comprehensive research works on the optimal allocation of Type 1 DGs. Singh et al. (2008) have carried out DG placement using genetic algorithm (GA) in the IEEE 16-bus, 37-bus and 75-bus radial distribution networks with different loading conditions. However, GA requires more computational time while suffering from premature convergence. Multi-objective particle swarm optimization (PSO) for DG placement in the IEEE-33-bus radial distribution system (RDS) has been proposed by Ameli et al. (2014) for power loss reduction, improvement of voltage profile and stability. Gomez-Gonzalez et al. (2012) have employed discrete PSO for optimal DG allocation to reduce power losses in the IEEE 30-bus radial distribution network. A hybrid GA-PSO-based algorithm for optimal DG allocation to reduce power losses and improve voltage profile and stability has been presented in Moradi and Abedini (2012). A multi-objective, modified honey bee mating optimization algorithm for siting and sizing of DG has been reported in Niknam et al. (2011). The proposed method avoids strong local convergence as compared to the original honey bee mating optimization algorithm. Several nature-inspired algorithms have also been proposed by researchers for siting and sizing of DGs. Some notable ones include the chaotic symbiotic organism search (CSOS) algorithm (Saha and Mukherjee 2016) and the artificial bee colony (ABC) algorithm (Abu-Mouti and El-Hawary 2011). Sheng et al. (2016) have implemented multi-objective harmony search algorithm (HSA) for optimal DG allocation in the 33-bus RDS. TLBO method for the optimal siting and sizing of DGs has been reported in Mohanty and Tripathy (2016). A multi-objective, modified teaching–learning-based optimization algorithm for the optimal allocation of DGs in the 33-bus, 69-bus and 118-bus RDS has been presented in Martín García and Gil Mena (2013).

1.1 Motivation and aim

Although analytical methods have no convergence issues, with an increase in the number and type of DGs, their complexity increases, with a consequent increase in the computational time. This is particularly true for multi-objective formulations with a large number of equality and inequality constraints. Analytical approaches for optimal DG allocation in distribution systems require more robust algorithms (Arqub and Abo-Hammour 2014; Abu Arqub et al. 2016; Arqub et al. 2017; Abu Arqub 2017) to solve differential and nonlinear equations. In this respect, heuristic methods for siting and sizing of DGs do not involve differential equations. However, the algorithms need to be tuned properly to reach the global solution for DG sizing and placement. Recently, TLBO method (Rao et al. 2011) has been developed which is almost independent of the optimization parameters and possesses excellent convergence characteristics for lesser number of variables. However, it has the tendency to be trapped in strong local minima when the number of variables increases. A modified TLBO algorithm for DG placement has been reported in Martín García and Gil Mena (2013) where additional mutation phase is considered for finding the global solution. Sultana and Roy (2014) have presented a quasi-oppositional TLBO (QOTLBO) for DG placement in RDS. However, these features add complexity to the TLBO and increase the computational time. An improved TLBO has been reported in Kanwar et al. (2015) in which a crossover rate and a crossover parameter have to be specified. However, both of them need to be tuned to achieve a satisfactory convergence. Harmony search (HS) is another swarm intelligence algorithm which shows good exploration capability but poor exploitation capability for global solutions. Several HS variants have been suggested to solve complex optimization problems, such as SGHS (Self-Adaptive Global Harmony Search Algorithm) (Pan et al. 2010), IHS (Mahdavi et al. 2007), ITHS (Intelligent Tuned Harmony Search algorithm) (Yadav et al. 2012), EHS (Enhanced Harmony Search) (Das et al. 2011), NGHS (Nobel Global Harmony Search) (Zou et al. 2010), DIHS (Tuo et al. 2015), NDHS (Chen et al. 2012) and DSHS (Kattan and Abdullah 2013). However, these improved versions of HS are also unable to handle complex optimization problems of high dimensionality and modality. IHS lacks in precise solution. It is observed that NGHS, SGHS and NDHS get easily trapped into strong local minima/maxima. Although solutions provided by EHS and DSHS are satisfactory, they require more convergence time for global solution with high-dimensional problems. It is observed that TLBO exhibits good search space exploitation capability while HS has good exploration capability. So, a proper integration of the merits of TLBO and HS would result in a better optimization technique for high-dimensional and multimodality problems.

To get a good balance of exploration and exploitation of the search space, a new optimization algorithm based on the hybridization of HS and TLBO is presented in this paper. In this algorithm, at first the HS algorithm is utilized to explore the search space with a high probability of finding the global solution. Subsequently, TLBO carries out exploitation of the search space for the global solution. For choice of TLBO or HS, the proposed algorithm uses self-adaptive selection probability.

In this work, at the outset, the performance of the proposed algorithm is tested on standard mathematical benchmark functions. Subsequently, a multi-objective problem of optimal DG allocation in the IEEE 33-bus, 69-bus and 118-bus RDS is solved by the ε-constraint method using HTLBO. The proposed HTLBO is compared with existing TLBOs and QOTLBO. The results validate the proposed method.

The contribution of the paper can be summarized as follows:

- Development of a HTLBO algorithm which is competent in handling continuous as well as discrete variables with constrained and unconstrained optimization problems.
- HTLBO utilizes the exploration quality of HS and the exploitation quality of TLBO. It has the capability to escape strong local maxima/minima convergence, thus yielding a global solution.
- A comparative analysis for solving multi-objective problems based on two approaches—the weighted sum and the ε-constraint method—is presented. The later is independent of penalty coefficients.
- HTLBO is validated with standard mathematical benchmark functions (both single- and multi-objective). The results are compared with global best ABC (g-ABC), parallel ABC (P-ABC) and improved TLBO (ITLBO) for single-objective functions. On the other hand, for multi-objective functions, the results are compared with NSGA-II.
- The impact of parameter variations of the proposed algorithm on the solution is investigated, which shows that proper tuning of algorithm parameters is required for global solution.
- Optimal siting and sizing of DGs is analyzed in the IEEE 33-bus, 69-bus and 118-bus radial distribution test systems to improve the network active power losses, voltage profile and voltage stability index.

1.2 Paper layout

The paper is organized as follows. Section 2 presents the mathematical problem formulation of the work carried out in this paper. Section 3 illustrates the basics of TLBO and HS algorithms. Section 4 presents several modifications carried out in the TLBO and HS algorithms to improve their performance. Section 5 illustrates the flowchart of the proposed HTLBO. Section 6 demonstrates the effectiveness and validity of the proposed HTLBO on mathematical benchmark function. The simulation results of DG allocation in various distribution networks are also presented in this section. Finally, conclusions are presented in Sect. 7.

2 Problem formulation

The proposed work has considered the following assumptions:

a. All RDS are balanced.
b. Unity power factor DGs have been employed in RDS.
c. Nominal load level and constant power load model is assumed.
d. The outputs of all DGs are time invariant.

2.1 Single-objective function (SOF)

The objective of allocation of DGs in RDS is to reduce the network active power losses and enhance the voltage profile and VSI while satisfying all working constraints. Descriptions of these SOF are given below:

2.1.1 Real power loss P_{loss}

The real power loss of the network is the primary concern while allocating DGs in RDS. Various formulations (Das et al. 1994; Teng 2003; Goswami and Basu 1991) exist in the literature for load flow studies of RDS. The P_{loss} can be calculated as shown below (Gözel and Hocaoglu 2009):

$$P_{\text{loss}} = \sum_{j=1}^{\text{nb}} I_j^2 R_j \quad \text{where} \quad I_j = \sum_{k=1}^{m} \left(\left(P_{L,k} - P_{DG,k}\right)^2 + Q_{L,k}^2 \right) / |V_k^2| \tag{1}$$

So, SOF to minimize real power loss is shown below:

$$F_1 = \text{Minimize } P_{\text{loss}} \tag{2}$$

In Eq. (1), $P_{L,k}$ and $Q_{L,k}$ are the real and reactive load demand at the kth bus, $P_{\text{DG},k}$ is the real power injected by the DG at the kth bus, '$|V_k|$' is the voltage magnitude at the kth bus, 'R_j' is the resistance of the jth line, 'n' is the total number of buses in the network, 'nb' is the total number of branches in the network and 'm' is the number of buses beyond branch 'j.'

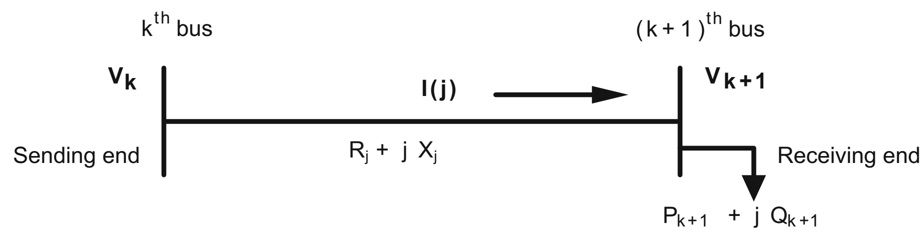

Fig. 1 Equivalent circuit of the jth branch of the network between buses 'k' and '$(k+1)$'

2.1.2 Voltage profile

It is desirable to keep the voltage magnitude (V_{k}) at a bus between 1.05 p.u. (maximum) and 0.95 p.u. (minimum). Real power injections by DGs allocated optimally enhance the voltage profile of the RDS. So, SOF (F_2) to minimize voltage deviation index (VDI) is formulated as shown below:

$$F_2 = \sum_{k=1}^{n} (V_k - V_{\text{rated}})^2,$$

where 'V_{k}' and 'V_{rated}' are expressed in p.u.

2.1.3 Voltage stability index (VSI)

The characterization of voltage profile of RDS is analyzed by its VSI. For stable operation of the network, the VSI must be greater than zero. So, VSI should be maximum to ensure maximum stability of RDS. The VSI formulation of a RDS is represented by Eq. (4) (Chakravorty and Das 2001) and is shown in Fig. 1.

$$VSI_{k+1} = |V_k|^4 - 4\{P_{k+1}X_j - Q_{k+1}R_j\}^2 - 4\{P_{k+1}R_j + Q_{k+1}X_j\}|V_k|^2 \tag{4}$$

The SOF (F_3) to maximize the VSI is shown below:

$$F_3 = \text{maximize VSI}, \tag{5}$$

where VSI_k and VSI_{k+1} are the VSI of the kth and $(k+1)$th bus, respectively and 'R_j' and 'X_j' denote the resistance and reactance, respectively, of the branch 'j' incorporated between the kth and the $(k+1)$th nodes as shown in Fig. 1a. Similarly, 'P_{k+1}' and 'Q_{k+1}' are the real and reactive power demands, respectively, at the $(k+1)$th node of the RDS.

2.2 Multi-objective function

A multi-objective function (MOF) considers all the objective functions simultaneously for either maximization or minimization, while satisfying the equality and inequality constraints. In this paper, a MOF (Sultana and Roy 2014) simultaneously minimizes power loss (F_1) and VDI (F_2) and maximizes VSI (F_3) by the ε-constraints method (Deb 2001), satisfying operational constraints like bus voltage limits, line thermal limits, DGs penetration limits and network power balance as given below:

$$\text{MOF} = \text{Minimize } f\mu(x) \tag{6}$$

$$\text{Subject to } f_m(x) \le \varepsilon_m \quad m = 1, 2, 3 \ldots. \text{ and } m \ne \mu;$$
$$g_j(x) \ge 0, \quad j = 1, 2, 3 \ldots.;$$
$$h_l(x) = 0, \quad l = 1, 2, 3 \ldots.;$$
$$x_i^{(L)} \le x_i \le x_i^{(U)}, i = 1, 2, 3 \ldots.;$$

where one of the objectives of the MOF is maximized/minimized, keeping the remaining objectives as constraints. Here, $f\mu(x)$ is the power loss while $f_m(x)$ comprises both the VDI and the inverse of VSI as constraints. The parameter ε_m represents the upper bound of the value of f_m. g_j comprise the bus voltage limits, line thermal limits, DGs penetration limits while h_k constitutes equality constraints (i.e., power balance), respectively. $x_i^{(L)}$ and $x_i^{(U)}$ are the variables' lower and upper limits, respectively.

2.2.1 Equality constraints

The SOF and the MOF are subject to the following constraints for the optimal allocation of DGs in the RDS as given below.

2.2.2 Active and reactive power balance constraints

$$P_{\text{sub}} + P_{\text{DG}} = P_{\text{loss}} + P_{\text{D}} \quad \text{and} \quad Q_{\text{sub}} + Q_{\text{DG}} = Q_{\text{loss}} + Q_{\text{D}} \tag{7}$$

$$Q_{\text{loss}} = \sum_{j=1}^{\text{nb}} I_j^2 X_j \tag{8}$$

where $P_{\text{sub}}/Q_{\text{sub}}$ are the active/reactive powers supplied by the substation, $P_{\text{D}}/Q_{\text{D}}$ are the total active/reactive power demands of the load and Q_{loss} is the reactive power loss in the distribution network.

2.2.3 Voltage limit constraint

The voltage magnitudes (V_k) of all the buses of RDS must be within limits of $V_{\max}$ (1.05 p.u.)) and $V_{\min}$ (0.95 p.u.)

$$V_{\min} \le V_k \le V_{\max} \quad k = 1, 2, 3, 4 \ldots n \tag{9}$$

2.2.4 Thermal limit (Kanwar et al. 2017)

$$I_j \leq I_j^{\max} \quad j = 1, 2, 3, 4 \ldots \mathrm{nb} \tag{10}$$

where I_j and $I_j^{\max}$ are the actual and the permissible loading of the branch 'j' of RDS.

2.2.5 Real power limit and reactive power limit (Moravej and Akhlaghi 2013)

$$P_{DG,k}^{\min} \leq P_{DG,k} \leq P_{DG,k}^{\max} \tag{11}$$

$$Q_{DG,k}^{\min} \leq Q_{DG,k} \leq Q_{DG,k}^{\max} \tag{12}$$

where $P_{\mathrm{DG},k}^{\min}$ and $P_{\mathrm{DG},k}^{\max}$ are the minimum and maximum injected active power limits, respectively, of the kth DG while $Q_{\mathrm{DG},k}^{\min}$ and $Q_{\mathrm{DG},k}^{\max}$ are the minimum and maximum injected reactive power limits, respectively, of the kth DG.

2.2.6 Maximum penetration of DG units in the system (Zhang et al. 2015)

$$\sum_{k=1}^{n} P_{\mathrm{DG},k} = \%J * \sum_{k=1}^{\mathrm{nb}} P_{L,k}, \tag{13}$$

where J is maximum penetration of DGs in the RDS.

2.3 TLBO algorithm

TLBO algorithm was first introduced by Rao et al. (2011). TLBO is a nature-inspired algorithm and is comprised of two stages, i.e., *Teaching phase and Learning Phase.* In '*teaching phase*', the best learner, i.e., teacher, transfers his knowledge to the other remaining learners to enhance their knowledge. Subsequently, in the '*learning phase*', each learner interacts with other fellow learners to further improve his/her own knowledge. These two stages are repeated till the TLBO proceeds toward the global best knowledge (global solution).

2.3.1 Teaching phase

The teacher keeps on trying to transfer his knowledge to the remaining learners, to the best of his capacity. Transfer of the teacher's knowledge can be utilized to improve the remaining learners/variables. It is mathematically expressed by Eq. (14). This can be illustrated with an example that to fulfill the objective of improving the knowledge of the students of a particular class in a particular subject. The student having the maximum marks is considered as the teacher ($X_{\mathrm{Teacher},i}$). The teacher's duty is to improve the old marks ($X_{\mathrm{old},i}^{\mathrm{HMS}}$) of other students to new marks ($X_{\mathrm{new},i}^{\mathrm{HMS}}$) toward the mean marks (M_i) of that particular subject/variables utilizing his own marks ($X_{\mathrm{Teacher},i}$). So, a random process takes place to improve the marks of the remaining students of the class. For each individual, new marks are generated by:

$$X_{\mathrm{new},i}^{\mathrm{HMS}} = X_{\mathrm{old},i}^{\mathrm{HMS}} + \mathrm{rand} * \left(X_{\mathrm{Teacher},i} - T_{\mathrm{F}} M_i\right), \tag{14}$$

where 'T_F' is defined as 'Teaching factor' which is randomly selected as either 1 or 2 (Rao et al. 2011). The newly generated solution vector (X_{new}) is accepted if its fitness (marks) is better than the old solution vector. In Eq. (14), $X_{\mathrm{old},i}^{\mathrm{HMS}}$ and $X_{\mathrm{new},i}^{\mathrm{HMS}}$ are the old and the new variables, respectively, while 'rand' is a randomly generated number between 0 and 1.

2.3.2 Learner phase

Learners' knowledge can be further improved by one's own effort. Students of the class coordinate with each other randomly which enhances their perceptive about a particular subject. Mathematically, the learner phase can be explained as per Eqs. (15, 16):

$$X_{\mathrm{new},i}^{\mathrm{HMS}} = X_{\mathrm{old},i}^{\mathrm{HMS}} + \mathrm{rand} * \left(X_j - X_k\right) \quad \text{if } F\left(X_j\right) < F(X_k), \tag{15}$$

$$X_{\mathrm{new},i}^{\mathrm{HMS}} = X_{\mathrm{old},i}^{\mathrm{HMS}} + \mathrm{rand} * \left(X_k - X_j\right) \quad \text{if } F\left(X_j\right) > F(X_k), \tag{16}$$

where 'i', 'j', 'k' are different learners in the class. $F(X)$ shows the fitness/knowledge (marks) of a particular learner in a subject. If the fitness corresponding to the set of '$X_{\mathrm{new},i}^{\mathrm{HMS}}$' is better than that corresponding to the set of '$X_{\mathrm{old},i}^{\mathrm{HMS}}$', a set of $X_{\mathrm{new},i}^{\mathrm{HMS}}$ is considered; otherwise, it is discarded.

So these two phases, i.e., teaching and learning phases, constitute an iteration. Several iterations of knowledge transferring and sharing ensure the global solution/best knowledge by the TLBO algorithm. Although this algorithm is almost parameter independent compared to other population-based optimization techniques, premature convergence may occur due to strong local maxima/minima trappings for multimodal problems.

2.4 Harmony search algorithm (HSA)

HSA mimics the improvisation of music players. The sounds for better aesthetic estimation can be improved through more and more practice just as the value of an objective function improves iteration by iteration.

The steps of the HSA are as follows:

Step 1 Initialize the harmony memory (HM) and algorithm parameters

At the beginning, a matrix of HM is formed, where each row represents a set of decision variables ($X_{\mathrm{new},i}^{\mathrm{HMS}}$) for the objective function $F\ (X_{\text{new},i}^{\text{HMS}})$ defined for the optimization problem. Each decision variable $X_{\text{new},i}^{\text{HMS}}$ is computed using Eq. (17).

$$X_{\text{new},i}^{\text{HMS}} = X_{i\,\text{min}} + \text{rand} * (X_{i\,\text{max}} - X_{i\,\text{min}}) \quad \forall i, = 1, 2, 3 \ldots N \text{ (number of variables)}, \tag{17}$$

where $X_{i\,\text{min}}$ and $X_{i\,\text{max}}$ are the minimum and the maximum value of marks (variable), respectively.

Harmonic memory size (HMS) represents numbers of the set of decision variables in HM, harmony memory consideration rate (HMCR) represents the probability of the new value of decision variables for HM, pitch adjustment rate (PAR) represents the probability of shifting the decision variables to neighboring values within the possible range and NI represents the stopping criterion.

$$\text{HM} = \begin{bmatrix} X_1^1 & X_2^1 & X_3^1 & \cdots X_{N-1}^1 & X_N^1 \\ X_1^2 & X_2^2 & X_3^2 & X_{N-1}^2 & X_N^2 \\ \vdots & \vdots & \vdots & \cdots \vdots & \vdots \\ X_1^{\text{HMS}-1} & X_2^{\text{HMS}-1} & X_3^{\text{HMS}-1} & \cdots X_{N-1}^{\text{HMS}-1} & X_N^{\text{HMS}-1} \\ X_1^{\text{HMS}} & X_2^{\text{HMS}} & X_3^{\text{HMS}} & X_{N-1}^{\text{HMS}} & X_1^{\text{HMS}} \end{bmatrix} \tag{18}$$

Step 2 Improvise new harmony

A new set of decision variables is generated based on the three parameters: (1) HMCR, (2) PAR and (3) random selection. The generation of the new decision variable of HM is known as improvisation. The probability of HMCR varies between 0 and 1. It is the probability of choosing the variable value from the HM, while (1-HMCR) is the probability of selecting the variable from the possible range of values, as given below:

if rand < HMCR

$$X_{\text{new},i}^{\text{HMS}} \leftarrow X_{\text{old},i}^{\text{HMS}} \in \left\{ X_i^1 \ \ X_i^2 \cdots \cdots\cdots X_i^{\text{HMS}} \right\} \tag{19}$$

else

$$X_{\text{new},i}^{\text{HMS}} = X_{i\,\text{min}} + \text{rand} * (X_{i\,\text{max}} - X_{i\,\text{min}}) \quad \text{where}$$

$i, = 1, 2, 3 \ldots N$

end (20)

HMCR decides whether to adjust the pitch of each decision variable or not. After considering the decision variable by HMCR, the pitch adjustment is decided by PAR as given below:

if rand < PAR

$$X_{\text{new},i}^{\text{HMS}} \leftarrow X_{old,i}^{HMS} + rand * BW \tag{21}$$

Else

$$X_{\text{new},i}^{\text{HMS}} \leftarrow X_{\text{old},i}^{\text{HMS}} - \text{rand} * \text{BW}$$

end (22)

where BW is known as the bandwidth. The value of BW lies between 0 and 1.

Step 3 Update harmony memory

If the new set of decision variables, i.e.,

$$X_{\text{new}}^{\text{HMS}} = \left\{ X_1^{\text{HMS}} \ \ X_2^{\text{HMS}} \cdots \cdots\cdots X_N^{\text{HMS}} \right\} \tag{23}$$

gives better objective function F $(X_{\text{new}}^{\text{HMS}})$ values than the worst set of decision variables in HM, the worst set of decision variables is replaced by the new set of decision variables.

Step 4. Termination

The HSA keeps on repeating steps 1, 2 and 3, till maximum number of improvisation (NI) is met, which is set during the parameter initialization process.

There are several modifications proposed in TLBO and HS, so that the individual algorithm has better exploration and exploitation capabilities before hybridization of TLBO and HS is carried out.

3 Alterations in the TLBO and HS algorithms

3.1 Alterations in the TLBO algorithm

The following alterations are adopted to enhance the global convergence of the TLBO and evade strong local minima/maxima trapping.

3.1.1 Alteration in teaching phase

In basic TLBO, the new set of variables is based on the mean marks of the particular subject and the teacher's knowledge. In the suggested algorithm, the solution vector with the worst fitness is considered instead of the mean (M_i). This ensures knowledge improvement of the weakest student of the class, resulting in better knowledge transfer to every student of the class. Thus, the new generated vector '$X_{\text{new},i}^{\text{HMS}}$' will have a higher probability of reaching the global solution/knowledge.

This modification can be mathematically represented by Eq. (24):

$$X_{\text{new},i}^{\text{HMS}} = X_{\text{old},i}^{\text{HMS}} + \text{rand} * \left(X_{\text{Teacher},i} - T_{\text{F}} X_{\text{worst},i}\right), \tag{24}$$

where $X_{\text{worst},i}$ is the vector having the worst fitness function within the population.

3.1.2 Alteration in T_F

'T_F' is randomly considered as 1 or 2; i.e., knowledge transferred from the best learner (teacher) to the remaining learner is either 0% or 100%, respectively. But practically knowledge transfer could be in between 0–100%. Hence, the 'T_F' is altered between 0 and 1, to account for practical knowledge transfer, as given below:

$$T_F = \left(1/_{\text{rand}}\right)^a, \tag{25}$$

where 'a' is defined as the teaching factor rate. High value of 'a' ensures larger search space which increases the probability of reaching the global solution. It is observed from several case studies (Sect. 6) that the value of 'a' between 0–5 ensures global solution.

3.1.3 Alteration in the HS algorithm

In basic HSA, the parameters HMCR, PAR and BW are constant values. The proposed algorithm adopts dynamic strategies to select the values of HMCR and PAR (Yadav et al. 2012). Dynamic selection of HMCR and PAR provides better balance in exploration and exploitation of search space in the hybrid algorithm:

$$\text{HMCR} = \text{HMCR}_{\max} - (\text{HMCR}_{\max} - \text{HMCR}_{\min}) * \left(\frac{\text{current iteration}}{\text{max iteration}}\right), \tag{26}$$

$$\text{PAR} = \text{PAR}_{\max} - (\text{PAR}_{\max} - \text{PAR}_{\min}) * \left(\frac{\text{current iteration}}{\text{max iteration}}\right), \tag{27}$$

$$\text{BW} = \text{BW}_{\max} * \exp\left[\ln\left(\frac{\text{BW}_{\max}}{\text{BW}_{\min}}\right) * \frac{\text{current iteration}}{\text{max iteration}}\right], \tag{28}$$

where $\text{HMCR}_{\min}$ and $\text{HMCR}_{\max}$ are the minimum and the maximum values of HMCR, respectively, $\text{PAR}_{\min}$ and $\text{PAR}_{\max}$ are the minimum and the maximum values of PAR, respectively, while $\text{BW}_{\min}$ and $\text{BW}_{\max}$ are the minimum and maximum values of BW, respectively.

4 Proposed HTLBO algorithm

It is observed that the characteristics of TLBO and HS algorithms are complimentary to each other; i.e., HSA has excellent exploratory behavior but slow convergence while TLBO exhibits very good exploitation characteristics and fast convergence. Hence, the proposed method aims to utilize the merits of both algorithms and reach the global solution quickly. So, for the maximum exploration of the search space, initially, HSA is employed and then exploitation of the search space is done with the help of TLBO. In the proposed method, selection of the teaching phase of the TLBO algorithm and local pitch adjustment by HMCR of HSA are based on the ratio autoselection rate (ASR) defined as

$$\text{ASR} = \frac{\text{Best fitness of HM}}{\text{Worst fitness of HM}} \tag{29}$$

As the value of ASR changes in each iteration, ASR is dynamic in nature and is self-adaptive for the selection of either of these two algorithms for the improvisation of the harmony vector. For minimization problems, as the value of best fitness will always be less than the worst fitness value, ASR will be less than 1. For maximization problems, ASR is obtained by minimizing the inverse of the fitness function values, which will also lead to ASR less than 1. Initially, ASR will be low which gives preference to the HS algorithm for better exploration of the search space. As ASR moves toward unity, teaching phase is selected for better tuning of the variables.

To minimize the demerits of HS and TLBO, the HTLBO initially utilizes the exploration characteristics of HS. Subsequently, the TLBO algorithm is implemented for better tuning and fast convergence of the solution vector. The following steps are considered for the HTLBO algorithm.

A. Target vector selection: $X_{\text{new}}^{\text{HMS}} = X_{\text{old}}^{\text{HMS}}$ is the harmony vector.
B. Generation of target vector $X_{\text{new},i}^{\text{HMS}}$ in each iteration is comprised of four steps.

Step 1 Autoselection rate

The selection of teaching phase or HMCR for the generation of target vector $X_{\text{new}}^{\text{HMS}}$ depends upon the *autoselection rate*. ASR is found using Eq. (29).

Step 2 Teaching phase/harmony memory consideration rate and local pitch adjustment/mutation phase

When ASR is less than 'r', ('r' is a number between 0 and 1), the teaching phase is selected and Eq. (24) is used to generate $X_{\text{new},i}^{\text{HMS}}$. If ASR is more than '$r$,' HS algorithm is selected for the generation of $X_{\text{new}}^{\text{HMS}}$. The probability of tuning the target vector is decided by the HMCR. If the random number is less than HMCR, local pitch adjustment of $X_{\text{new},i}^{\text{HMS}}$ is carried out by using Eq. (27); otherwise, mutation phase is carried out according to Eq. (20) to generate the new target vector $X_{\text{new}}^{\text{HMS}}$ in the feasible space. If the fitness of the target vector $X_{\text{new}}^{\text{HMS}}$ is better than that of the worst fitness vector, then $X_{\text{worst},i}$ is replaced by $X_{\text{new}}^{\text{HMS}}$.

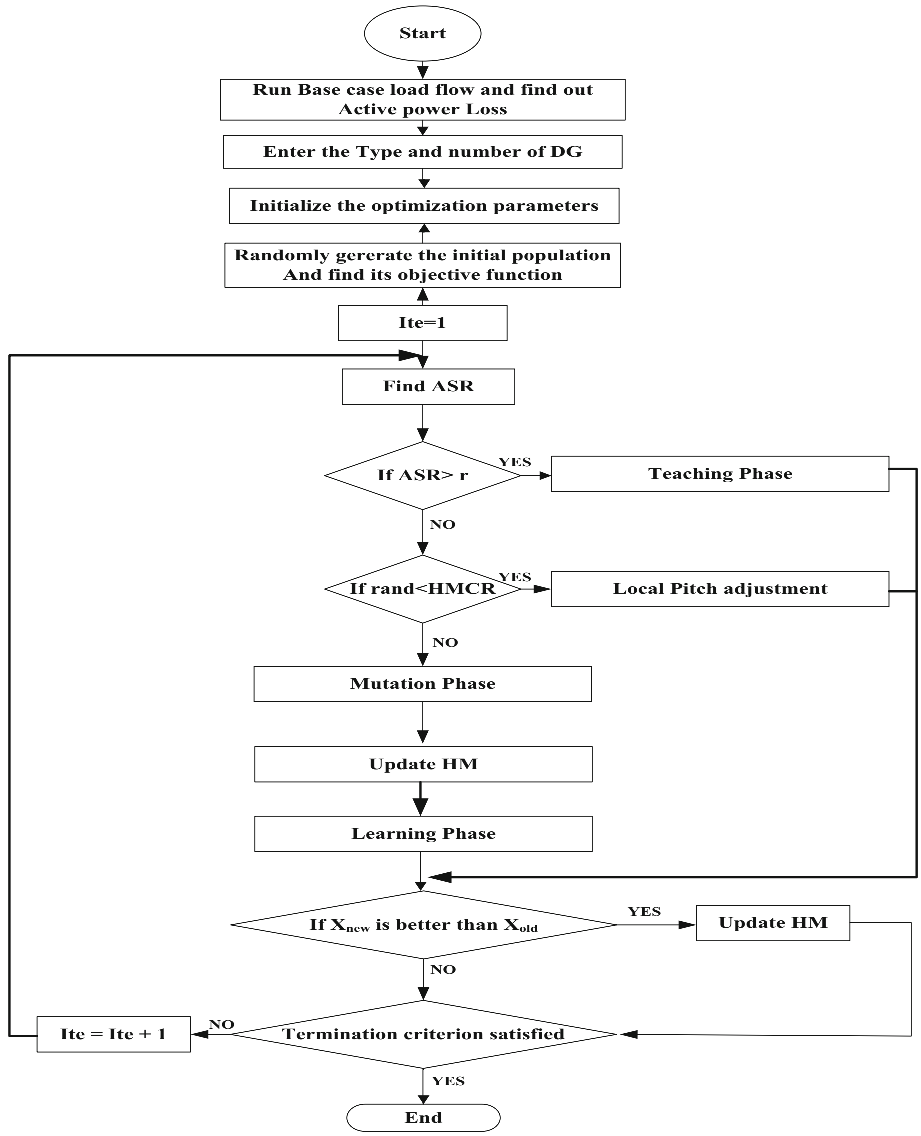

Fig. 2 Flowchart for the proposed HTLBO algorithm

Step 3 Learning phase

This phase enhances the knowledge (fitness) of the target vector $X_{\text{new},i}^{\text{HMS}}$ by interacting with the randomly selected harmony vector from harmony memory. Improvement of $X_{\text{new}}^{\text{HMS}}$ is done according to Eqs. (15, 16). If the fitness of the target vector $X_{\text{new}}^{\text{HMS}}$ is better than the fitness of the worst fitness vector, then $X_{\text{worst},i}$ is replaced by $X_{\text{new}}^{\text{HMS}}$.

Step 4 Dynamic adjustment of parameters

For the efficient operation of the HTLBO algorithm, the HMCR, PAR and the BW parameters are dynamically tuned, in each iteration, as per Eqs. (26), (27) and (28).

C. If the target vector generated has better fitness, then the HM is updated; otherwise, the next iteration is started. If the number of iterations satisfies the condition for termination, the algorithm is terminated and the best solution vector of HM is selected as the solution of the objective function.

The HTLBO algorithm parameters are detailed in Table 5.

The above steps of the proposed algorithm can be well understood by the flowchart shown in Fig. 2.

5 Case studies and results

The suggested HTLBO algorithm is first validated on standard mathematical benchmark functions. The HTLBO algorithm is tested for 20, 30 and 50 variables, and the results are shown in Table 1. Subsequently, the suggested HTLBO was used for optimal allocation of Type 1 DGs in the IEEE 33-bus, 69-bus and 118-bus RDS using ε-constraints method for the MOF. The MOF considers all the three SOFs simultaneously and results in better F_1, F_2 and F_3 than TLBO and

Table 1 Mathematical benchmark functions (Rao et al. 2011)

S. no.	Function	Formulation	D	Search range
1.	Sphere	$F(x)_{\min} = \sum_{i=1}^{D} x_i^2$	30	[− 100, 100]
2.	Schwefel 2.22	$F(x) = \sum_{i=1}^{D} \lvert x_i \rvert + \prod_{i=1}^{n} \lvert x_i \rvert$	30	[− 10, 10]
3.	Schwefel 1.2	$F(x) = \sum_{i=1}^{D} \left(\sum_{j=1}^{i} x_j \right)^2$	30	[− 100, 100]
4.	Schwefel 2.21	$F(x) = \max_{1 \le i \le D} \lvert x_i \rvert$	30	[− 100, 100]
5.	Rosenbrock	$F(x)_{\min} = \sum_{i=1}^{D} \left[100\left(x_i^2 - x_{i+1}\right)^2 + (1 - x_i)^2 \right]$	30	[− 2.048, 2.048]
6.	Step 2	$F(x) = \sum_{i=1}^{D} ([x_i + 0.5])^2$	30	[− 100, 100]
7.	Rastrigin	$F(x)_{\min} = \sum_{i=1}^{d} \left[x_i^2 - 10\cos(2\pi x_i) + 10 \right]$	30	[− 5.12, 5.12]
8.	Ackley	$F(x)_{\min} = -20e^{\left(-0.2\sqrt{\frac{1}{D}\sum_{i=1}^{D} x_i^2}\right)} - e^{\left(\frac{1}{D}\sum_{i=1}^{D}\cos(2\pi x_i)\right)} + 20 + e^1$	30	[− 32.768, 32.768]
9.	Griewank	$F(x)_{\min} = \frac{1}{4000}\sum_{i=1}^{D} x_i^2 - \prod_{i=1}^{D} \cos\left(\frac{x_i}{\sqrt{i}}\right) + 1$	30	[− 600, 600]
10.	Penalized	$F(x) = \frac{\pi}{D}\left[10\sin^2(\pi y_1) + \sum_{i=1}^{D-1} (y_i - 1)^2 \left\{ 1 + 10\sin^2(\pi y_{i+1}) \right\} + (y_D - 1)^2 \right] + \sum_{i=1}^{D} u(x_i, 10, 100, 4)$ $u(x_i, ak, m) = \begin{cases} k(x_i - a)^m, & x_i > a, \\ 0, & -a \le x_i \le a,\ y_i = 1 + 1/4(x_i + 1) \\ k(-x_i - a)^m & x_i < -a \end{cases}$	30	[− 50, 50]
11.	Penalized 2	$F(x) = \left[0.110\sin^2(\pi x_1) + \sum_{i=1}^{D-1} (x_i - 1)^2 \left\{ 1 + \sin^2(3\pi x_{i+1}) \right\} + (x_D - 1)^2 + \left(1 + sin^2(2\pi x_D) \right) \right] + \sum_{i=1}^{D} u(x_i, 5, 100, 4)$ $u(x_i, ak, m) = \begin{cases} k(x_i - a)^m, & x_i > a, \\ 0, & -a \le x_i \le a \\ k(-x_i - a)^m & x_i < -a \end{cases}$	30	[− 50, 50]

QOTLBO, respectively, as shown in subsequent tables. The proposed HTLBO algorithm was implemented in MATLAB R2015a environment on a Intel i5-4570, 3.2 GHz processor, 4 GB RAM, desktop PC.

5.1 Test case 1: Mathematical benchmark validation

The performance of the proposed HTLBO algorithm is validated on 11 mathematical benchmark test functions (Martín García and Gil Mena 2013) as given in Table 1. A comparison of the proposed HTLBO vis-à-vis other algorithms (Rao et al. 2011) is shown in Table 2. It is observed that the proposed method gives the best results with Penalized, Penalized 2 and Rosenbrock functions, while it yields results identical to ITLBO (improved TLBO) with Sphere, Schwefel 2.22, Schwefel 1.2, Griewank, Ackley and Rastrigin functions. However, it is observed that for the Schwefel 2.21 and Step 2 functions, ITLBO gives the best result. For the purpose of demonstration, Pareto sets are obtained for some multi-objective test functions (unconstrained and

Table 2 Comparative results of HTLBO algorithm with other algorithms (Rao et al. 2011) over 30 runs

F. no		G-ABC		PS-ABC		TLBO		ITLBO		HTLBO	
		Mean	SD	Mean	SD	Mean	SD	Mean	SD	Mean	SD
1	20	3.1943E−16	7.3909E−17	0.00	0.00	0.00	0.00	0.00	0.00	0.00	0.00
	30	6.2643E−16	1.0859E−16	0.00	0.00	0.00	0.00	0.00	0.00	0.00	0.00
	50	1.2546E−5	6.0511E−9	0.00	0.00	0.00	0.00	0.00	0.00	0.00	0.00
2	20	9.3611E−16	1.3278E−16	0.00	0.00	0.00	0.00	0.00	0.00	0.00	0.00
	30	1.3019E−10	4.6859E−11	0.00	0.00	0.00	0.00	0.00	0.00	0.00	0.00
	50	2.3671E−05	6.1889E−06	0.00	0.00	0.00	0.00	0.00	0.00	0.00	0.00
3	20	2.6919E3	1.4619E3	0.00	0.00	0.00	0.00	0.00	0.00	0.00	0.00
	30	1.0939E4	2.5670E3	0.00	0.00	0.00	0.00	0.00	0.00	0.00	0.00
	50	4.1236E4	5.8269E3	0.00	0.00	0.00	0.00	0.00	0.00	0.00	0.00
4	20	0.3325	1.0786	0.00	0.00	0.00	0.00	0.00	0.00	4.9407E−324	0.00
	30	12.6211	2.6556	8.59E−115	4.71E−114	4.9E−324	0.00	0.00	0.00	4.9407E−324	0.00
	50	45.3075	4.3151	19.6683	6.341E+00	9.9E−324	0.00	0.00	0.00	4.9407E−324	0.00
5	20	1.6769	2.9037	0.5190	1.0764	15.0536	2.28E−01	1.3785	8.49E−01	**0.1332**	**0.14021**
	30	7.47961	19.0926	1.5922	4.4066	25.4036	3.50E−01	15.032	1.2E+00	16.141	1.4042
	50	25.7164	31.75811	34.4913	30.3412	45.8955	2.89E−01	38.7294	7.57E−01	42.447	1.1164
6	20	3.3386E−16	1.0154E−16	2.6147E−16	3.8684E−17	9.24E−33	4.36E−33	0.00	0.00	0.00	0.00
	30	6.4499E−16	1.1126E−16	5.7169E−16	8.2549E−17	1.94E−29	1.88E−29	0.00	0.00	2.5063e−32	7.0518e32
	50	5.6529E−09	3.6854E−09	1.1674E−15	1.4114E−16	3.26E−13	5.11E−13	1.51E−32	8.89E−33	1.8917e−14	4.3031e−14
7	20	0.00	0.00	0.00	0.00	6.41E−14	6.16E−14	0.00	0.00	0.00	0.00
	30	3.3165E−02	1.8165E−01	0.00	0.00	6.95E−13	1.64E−12	0.00	0.00	0.00	0.00
	50	2.1733	1.0728	0.00	0.00	7.90E−13	1.89E−12	0.00	0.00	0.00	0.00
8	20	2.7533E−14	3.5832E−15	8.8817E−16	0.00	3.55E−15	8.32E−31	7.11E−16	0.00	2.2201e−15	0.00
	30	7.7828E−10	2.9817E−10	8.8817E−16	0.00	3.55E−15	8.32E−31	7.11E−16	0.00	2.2201e−15	0.00
	50	1.1137E−04	3.8873E−05	8.8817E−16	0.00	3.55E−15	8.32E−31	7.11E−16	0.00	2.2201e−15	0.00
9	20	6.0279E−04	2.2313E−03	0.00	0.00	0.00	0.00	0.00	0.00	0.00	0.00
	30	6.9655E−04	2.2609E−03	0.00	0.00	0.00	0.00	0.00	0.00	0.00	0.00
	50	1.0470E−03	2.7482E−03	0.00	0.00	0.00	0.00	0.00	0.00	0.00	0.00
10	20	3.2621E−16	6.6721E−17	2.5576E−16	4.9715E−17	4.00E−08	6.85E−24	2.42E−16	1.09E−16	**2.355e−32**	**8.4989e−48**
	30	5.8570E−16	1.1349E−16	5.5312E−16	8.6858E−17	2.67E−08	6.79E−12	4.98E−16	2.14E−16	**3.2337E−29**	**6.4289E−29**
	50	9.3017E−11	7.9664E−11	1.0252E−15	1.5815E−16	5.18E−05	1.92E−04	9.19E−16	5.38E−16	**3.4659E−16**	**2.9939E−16**
11	20	6.5528E−08	2.4413E−07	2.3456E−18	2.2088E−18	2.34E−08	6.85E−24	1.93E−18	1.12E−18	**1.3498E−32**	**0**
	30	2.1724E−07	5.6676E−07	6.0601E−18	5.6064E−18	2.37E−08	4.91E−10	5.92E−18	4.74E−18	**3.1884E−28**	**4.0023E−28**
	50	8.8776E−07	1.5324E−06	5.0541E−17	1.5350E−16	1.52E−03	5.29E−03	4.87E−17	4.26E−17	5.1175E−15	3.2346E−16

Bold indicates the better obtained result

Table 3 Mathematical benchmark functions for multi-objective functions (Deb 2001)

S. no.	Function	Objective function	D	Search range	Comment
1	SCH	$f_1(x) = x^2$ $f_2(x) = (x-2)^2$	1	$[-10^3, 10^3]$	Convex
2	KUR	$f_1(x) = \sum_{i=1}^{n-1}\left[-10\exp\left(-0.2\sqrt{x_i^2 + x_{i+1}^2}\right)\right]$ $f_2(x) = \sum_{i=1}^{n-1}\left(\lvert x_i\rvert^{0.8} + 5\sin x_i^3\right)$	3	$[-5, 5]$	Nonconvex
3	ZDT3	$f_1(x) = x_1$ $f_2(x) = g(x)[1 - \sqrt{x_1/g(x)} - \frac{x_1}{g(x)}\sin(10\pi x_1)$ $g(x) = 1 + 9\left(\sum_{i=2}^{n} x_i\right)/(n-1)$	30	[0, 1]	Convex, disconnected
4	ZDT4	$f_1(x) = x_1$ $f_2(x) = g(x)\left[1 - \sqrt{x_1/g(x)}\right]$ $g(x) = 1 + 10(n-1) + \sum_{i=2}^{n}\left[x_i^2 - 10\cos(4\pi x_i)\right]$	10	$x_1 \in [0, 1]$ $x_i \in [-5, 5], i = 2, 3 \ldots, n$	Nonconvex
5	BNH	$f_1(x) = 4x_1^2 + 4x_2^2$ $f_2(x) = (x_1-5)^2 + (x_2-5)^2$ Subject to $C_1(x) = (x_1-5)^2 + x_2^2 \le 25,$ $C_2(x) = (x_1-8)^2 + (x_2+3)^2 \ge 7.7$	2	$0 \le x_1 \le 5,$ $0 \le x_2 \le 3$	Convex
6	TNK	$f_1(x) = x_1$ $f_2(x) = x_2$ Subject to $C_1(x) = x_1^2 + x_2^2 - 1 - 0.1\cos\left(16\tan^{-1}(x_1/x_2)\right) \ge 0,$ $C_2(x) = (x_1-0.5)^2 + (x_2-0.5)^2 \le 0.5$	2	$0 \le x_1 \le \pi,$ $0 \le x_2 \le \pi$	Discontinuous
7	OSY	$f_1(x) =$ $-\left[25(x_1-2)^2 + (x_2-2)^2 + (x_3-1)^2 + (x_4-4)^2 + (x_5-1)^2\right]$ $f_2(x) = x_1^2 + x_2^2 + x_3^2 + x_4^2 + x_5^2 + x_6^2$ Subject to $C_1(x) = x_1 + x_2 - 2 \ge 0,$ $C_2(x) = 6 - x_1 - x_2 \ge 0$ $C_3(x) = 2 + x_1 - x_2 \ge 0$ $C_4(x) = 2 - x_1 + 3x_2 \ge 0$ $C_5(x) = 4 - (x_3-3)^2 - x_4 \ge 0$ $C_6(x) = (x_5-3)^2 + x_6 - 4 \ge 0$	6	$0 \le x_1, x_2, x_6 \le 10$ $1 \le x_3, x_5 \le 5$ $0 \le x_4 \le 6$	Continuous

constrained) shown in Table 3, when HTLBO is integrated with non-dominating sorting algorithm (Deb 2001). From Fig. 3a, it is observed that for unconstrained problems, HTLBO yields similar results with SCH and KUR, inferior results with ZDT3 and better results with ZDT4, as compared to NSGA-II (Deb 2001). For constrained problems, HTLBO gives similar result with TNK, while better results are obtained with BNH and OSY than NSGA-II, as shown in Fig. 3b. Table 4 shows the impact of variations of HTLBO parameters on the solution of the Sphere function. The parameters considered are the teaching factor rate 'a', HMS, maximum iteration (NI) and the number of variables (X). It is observed from Table 4 that for HMS = 10 and maximum iteration = 6000, HTLBO algorithm gives best results for all 'a.' Similarly, for HMS = 20 and 30, HTLBO gives best results with '$a = 0.2$.' For HMS = 40 and 50, HTLBO gives best results with '$a = 0.1$' while considering number of variables = 20. On the other hand, with number of variables = 30 and 50, '$a = 0.2$' gives better result.

5.2 Test case 2: Selection of optimal size and location of distributed generation (DG) resources in different RDSs

5.2.1 IEEE 33-bus RDS

The suggested HTLBO is first implemented for optimal allocation of DGs in the IEEE 33-bus RDS using two methods. The first one is the weighted sum method (Sultana and Roy 2014), where the MOF is formulated as a weighted sum of the three SOFs as detailed in 'Appendix.' The second approach comprises the modification of the MOF into a SOF using the ε-constraints method (Deb 2001). In both the methods, the objective is simultaneous minimization of the network active power losses and voltage deviation together with VSI maxi-

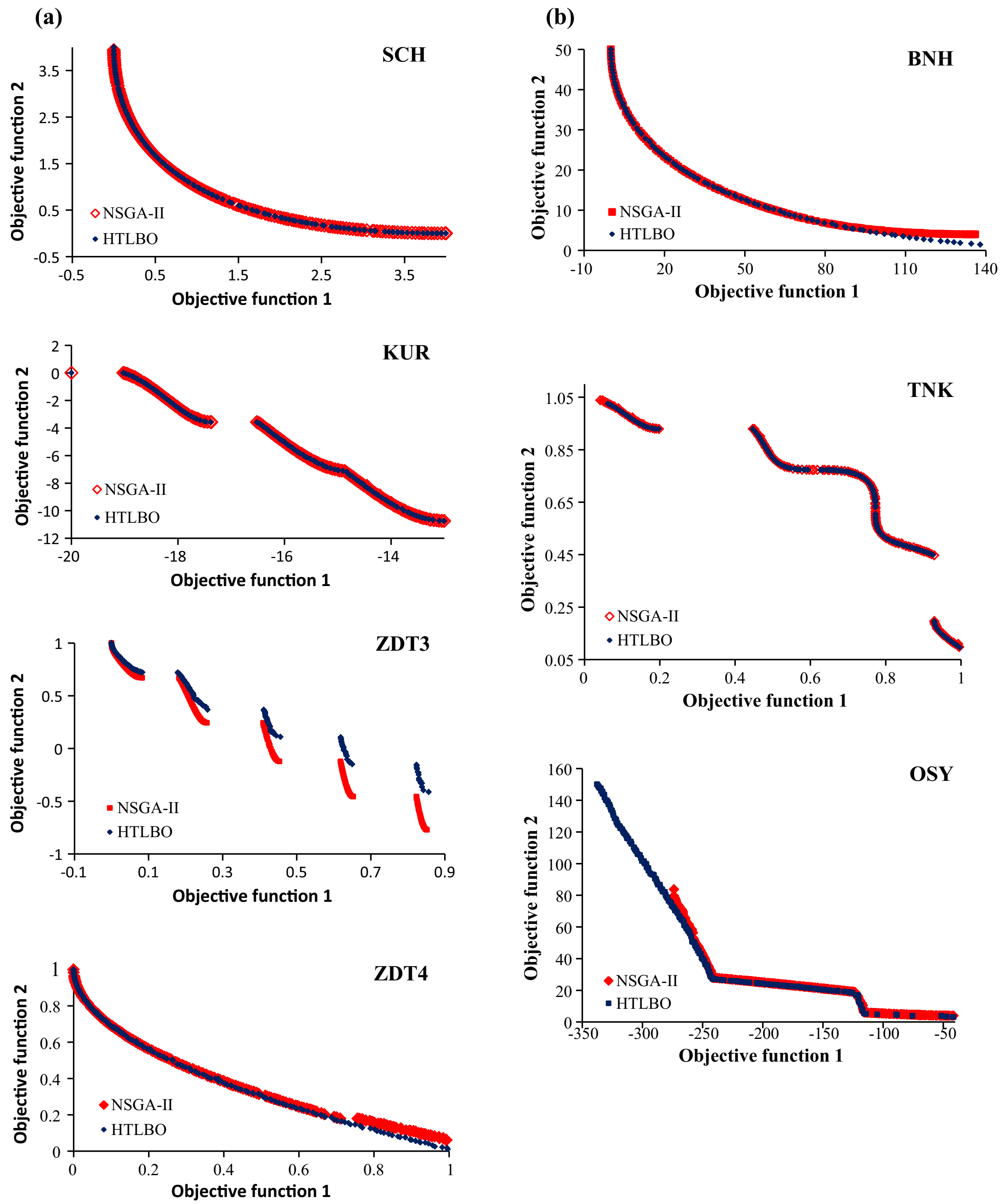

Fig. 3 **a** Comparative results of unconstrained multi-objective functions by NSGA-II and HTLBO for [1] SCH. [2] KUR. [3] ZDT3. [4] ZDT4. **b** Comparative results of constrained multi-objective functions by NSGA-II and HTLBO for [1] BNH. [2] TNK. [3] OSY

mization. The detailed network data are given in Baran and Wu (1989). It has 33 nodes, three laterals, 37 branches with five tie switches normally kept open. The nominal voltage rating is 12.66 kV. The nominal load demand of the RDS is 3.72 MW and 2.3 MVAr, respectively. The base case total active power losses are 210.998 kW while the total reactive power losses are 143 kVAr. The base case VSI of this RDS is 0.667168 (Injeti and Prema Kumar 2013). The network base KVA is 1000 KVA (Baran and Wu 1989). Three DGs (Type 1) are selected for optimal allocation in this RDS. The HTLBO parameters are selected as shown in Table 5.

The weight factors 'b_1', 'b_2' and 'b_3' (detailed in 'Appendix') corresponding to the three SOFs are shown in Table 6 (Sultana and Roy 2014). As shown in Table 6, when

Table 4 Impact of algorithm parameters on mathematical test functions over 30 runs

Sphere function (1)			Teaching factor rate(a)							
HMS	Maxite	Variables	0.1		0.2		0.3		0.4	
			Mean	SD	Mean	SD	Mean	SD	Mean	SD
10	6000	20	0	0	0	0	0	0	0	0
		30	0	0	0	0	0	0	0	0
		50	0	0	0	0	0	0	0	0
20	3000	20	1.32E−220	0	**3.11E−233**	**0**	8.64E−223	0	1.95E−198	0
		30	1.69E−174	0	**5.21E−191**	**0**	2.74E−174	0	6.10E−155	1.30E−154
		50	1.40E−142	1.97E−142	**1.47E−154**	**3.22E−154**	1.31E−141	2.92E−141	1.29E−120	2.37E−120
30	2000	20	2.61E−119	5.29E−119	**1.44E−121**	**2.99E−121**	4.18E−111	9.33E−111	5.53E−102	1.06E−101
		30	6.89E−90	9.66E−90	**3.00E−91**	**6.62E−91**	2.37E−84	5.28E−84	8.63E−76	9.88E−76
		50	5.96E−67	1.29E−66	**1.63E−73**	**3.27E−73**	8.72E−67	6.04E−67	3.53E−55	4.40E−55
40	1500	20	**5.72E−78**	**8.55E−78**	1.18E−76	2.45E−76	3.01E−71	4.27E−71	7.46E−64	1.64E−63
		30	2.65E−56	2.08E−56	**1.72E−57**	**1.28E−57**	5.83E−53	5.64E−53	5.94E−45	1.20E−44
		50	5.46E−39	1.16E−38	**1.15E−42**	**1.07E−42**	5.09E−38	9.58E−38	3.43E−32	2.45E−32
50	1200	20	**2.97E−55**	**3.02E−55**	4.81E−53	1.02E−52	5.80E−49	1.27E−48	1.29E−44	1.29E−44
		30	3.98E−38	2.64E−38	**5.34E−39**	**5.18E−39**	5.65E−35	6.93E−35	1.03E−30	1.24E−30
		50	9.07E−27	7.55E−27	**3.74E−28**	**5.55E−28**	2.53E−25	2.61E−25	1.32E−20	1.03E−20

Bold indicates the better obtained result
Where *Maxite* maximum iteration, *SD* standard deviation

Table 5 HTLBO algorithm parameters

Parameter	Values
a	0.2
$HMCR_{min}$	0.7
$HMCR_{max}$	0.95
PAR_{min}	0.3
PAR_{max}	0.5
r	0.9
BW_{min}	0.0001
BW_{max}	0.1
Maxiteration	500
HMS	90

$b_1 = 1.0$ $b_2 = 0.6$ and $b_3 = 0.0.35$, the suggested HTLBO shows reduction in the active power losses to 82.815 kW (from 210.998 kW in the base case). On the other hand, results of MOF with ε-constraints method give simultaneous improvement in all three SOFs, i.e., F_1, F_2 and F_3 (97.5330 kW, 0.0009 p.u. and 0.9653 p.u., respectively), in comparison with both TLBO and QOTLBO, as shown in Table 6. Figure 4a shows the voltage profile enhancement of the IEEE 33-bus RDS with DGs vis-a-vis that without DG. From Fig. 4a, minimum network voltage magnitude of 0.9836 p.u. at node 33 is noticed in the presence of DGs. The network voltage profile shows a remarkable improvement than that without DG (voltage magnitude of 0.9038 p.u. at bus 18).

Figure 3b shows the convergence characteristics of the MOF corresponding to the TLBO, QTLBO and the proposed HTLBO algorithm. It is observed from Fig. 4b that the proposed algorithm (HTLBO) has the lowest fitness value, i.e., 0.4590 p.u., and the fastest convergence rate.

5.2.2 69-bus RDS

The proposed algorithm (HTLBO) is now implemented on the IEEE 69-bus RDS for optimal allocation of DGs. Again, three DGs (Type 1) have been considered. Similar to the case of the IEEE 33-bus RDS above, the MOF (for minimization of the network active power losses and voltage deviation together with maximization of VSI) is evaluated using both the weighted sum method and the ε-constraints method. The HTLBO parameters are again selected as shown in Table 5. The detailed network data are given in Das et al. (1994). It has 69 nodes, seven laterals, 73 branches with five tie switches normally kept open. The nominal voltage rating is 12.66 kV. Nominal load demand on the RDS is 3.8 MW and 2.69 MVAr. The base case real and reactive power losses are 224.9 kW and 102.13 kVAr, respectively. The base case VSI of this RDS is 0.6833 (Injeti and Prema Kumar 2013). The network base is 1000 KVA (Baran and Wu 1989).

As shown in Table 7, when $b_1 = 1.0$, $b_2 = 0.6$ and $b_3 = 0.0.35$, HTLBO shows reduction in active power losses to 76.938 kW and improvement in the VDI to 0.0006 p.u. On the other hand, results of MOF with ε-constraints method give simultaneous improvement in all the three SOFs (F_1, F_2 and F_3) to 79.431 kW, 0.0003 p.u. and 0.9770 p.u., respectively, in comparison with both TLBO and QOTLBO, as shown in Table 6. Figure 5a shows the voltage profile enhancement of the IEEE 69-bus RDS with DGs over that without DG. From Fig. 5a, it is observed that the minimum network voltage

Table 6 Simulation results for optimal DG allocation in 33 BUS RDS using TLBO, QOTLBO and HTLBO

	TLBO (Sultana and Roy 2014)		QOTLBO (Sultana and Roy 2014)		HTLBO		HTLBO	
	Penalty factors ($b_1 = 1.0$, $b_2 = 0.6$, $b_3 = 0.0.35$)						ε-Constraints methods	
	Optimal DG		Optimal DG		Optimal DG		Optimal DG	
	Location	Size (MW)	Location	Size (MW)	Location	Size (MW)	Location	Size (MW)
	12	1.1826	13	1.0834	13	1.0229	13	1.2043
	28	1.1913	26	1.1876	25	0.9016	25	0.8573
	30	1.1863	30	1.1992	30	1.4567	30	1.6480
P_{loss} (kW)	124.695		103.403		82.815		**97.5330**	
VDI (p.u.)	0.0011		0.0011		0.0026		**0.0009**	
VSI^{-1}	1.0523		1.0493		1.0684		**1.0383**	
VSI	0.9503		0.9530		0.9360		**0.9653**	
MOF (p.u.)	0.4936		0.4713		0.4590		–	

Bold indicates the better obtained result

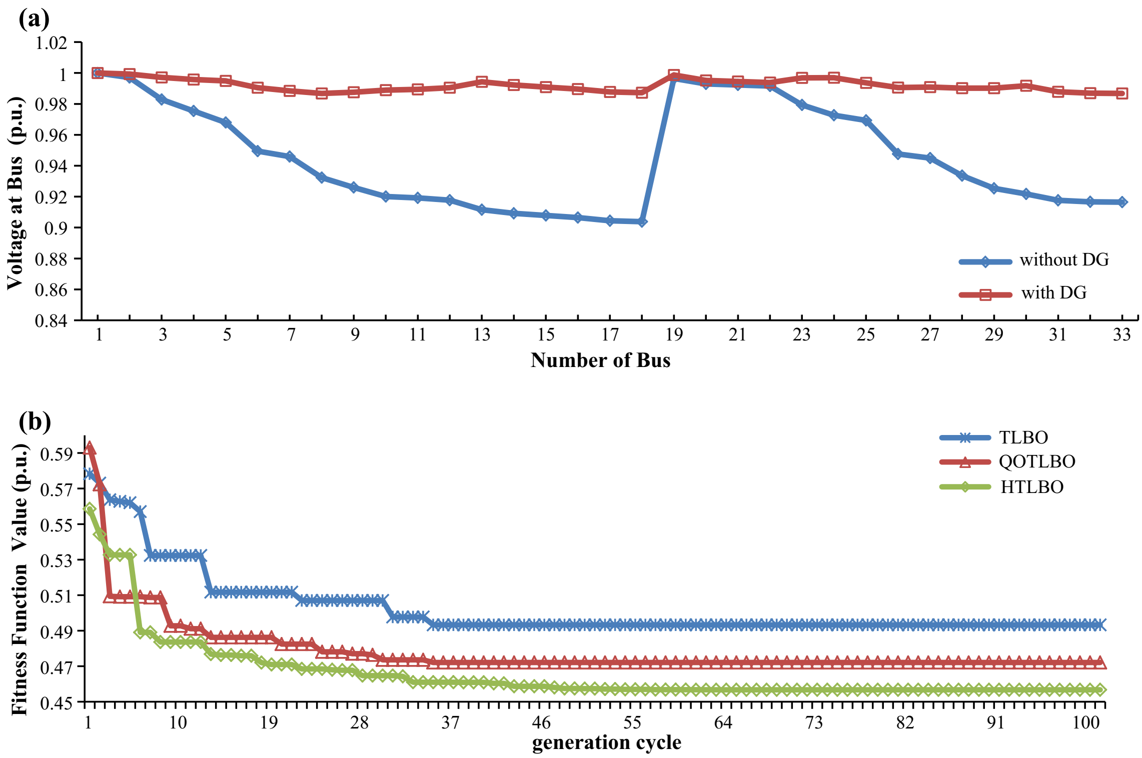

Fig. 4 **a** Bus voltage profile of the 33-bus radial distribution system without and with DG. **b** Convergence characteristics of 33-bus RDS for multi-objective function for TLBO, QOTLBO and HTLBO

magnitude of 0.9942 p.u. occurs at bus 56 in the presence of DGs. Thus, with DGs, the network voltage profile shows a remarkable improvement than that without DG (0.9092 p.u. at bus 65). Figure 5b shows the convergence characteristics of the MOF corresponding to the TLBO, QTLBO and the proposed HTLBO algorithm. It is observed from Fig. 5b that the proposed algorithm (HTLBO) has the lowest fitness value, i.e., 0.4389 p.u., and the fastest convergence rate.

5.2.3 118-bus RDS

The proposed algorithm (HTLBO) is now implemented on the IEEE 118-bus RDS for optimal allocation of DGs. Seven DGs (Type 1) have been considered. Similar to the case of the IEEE 33- and 69-bus RDS above, the MOF (for minimization of the network active power losses and voltage deviation together with maximization of VSI) is evaluated using both the weighted sum method and the ε-constraints method. The HTLBO parameters are again selected as shown in Table 5. The detailed network data are given in Zhang et al. (2007). It has 119 nodes, 16 laterals, 132 branches with 15 tie switches normally kept open. The nominal voltage rating is 11 kV. Nominal load demand on the RDS is 22.709 MW and 17.041 MVAr. The base case real and reactive power losses are 1298.0916 kW and 978.736 kVAr, respectively. The base case VSI of this RDS is 0.569734 (Injeti and Prema Kumar 2013). The network base is 100 MVA (Zhang et al. 2007).

As shown in Table 8, when $b_1 = 1.0$, $b_2 = 0.6$ and $b_3 =$ 0.0.35, HTLBO shows improvement in both VDI and VSI as compared to both TLBO and QOTLBO, although the active power losses are inferior to both TLBO and QOTLBO. On the other hand, results of MOF with ε-constraints method give simultaneous improvement in all the three SOFs (F_1, F_2 and F_3) to 658.756 kW, 0.0225 p.u. and 0.8978 p.u., respectively, in comparison with both TLBO and QOTLBO, as shown in Table 8. Figure 4a shows the voltage profile enhancement of the IEEE 118-bus RDS with DGs over that without DG.

From Fig. 6a, it is observed that the minimum network voltage magnitude of 0.97344 p.u. occurs at node 56 in the presence of DGs. The network voltage profile again shows a remarkable improvement over that without any DG (voltage magnitude of 0.86879 p.u. at bus 80). Figure 6b shows the convergence characteristics of the MOF corresponding to the TLBO, QTLBO and the proposed HTLBO algorithm. It is observed from Fig. 6b that the proposed algorithm (HTLBO) has the lowest fitness value of 0.4104 p.u.

Table 7 Simulation results for MOF using TLBO, QOTLBO and HTLBO of 69-bus RDS

	TLBO (Sultana and Roy 2014)		QOTLBO (Sultana and Roy 2014)		HTLBO		HTLBO	
	Penalty factors ($b_1 = 1.0$, $b_2 = 0.6$, $b_3 = 0.0.35$)						ε-Constraints methods	
	Optimal DG		Optimal DG		Optimal DG		Optimal DG	
	Location	Size (MW)	Location	Size (MW)	Location	Size (MW)	Location	Size (MW)
	13	1.0134	15	0.8114	12	0.9424	**12**	**0.9956**
	61	0.9901	61	1.1470	25	0.2306	**20**	**0.2398**
	62	1.1601	63	1.0022	61	2.0508	**61**	**2.1123**
P_{loss} (kW)	82.172		80.585		76.938		**79.431**	
VDI (p.u.)	0.0008		0.0007		0.0006		**0.0003**	
VSI^{-1}	1.0262		1.0236		1.0334		**1.0235**	
VSI	0.9745		0.9769		0.9677		**0.9770**	
MOF (p.u.)	0.4418		0.4393		0.4389		–	

Bold indicates the better obtained result

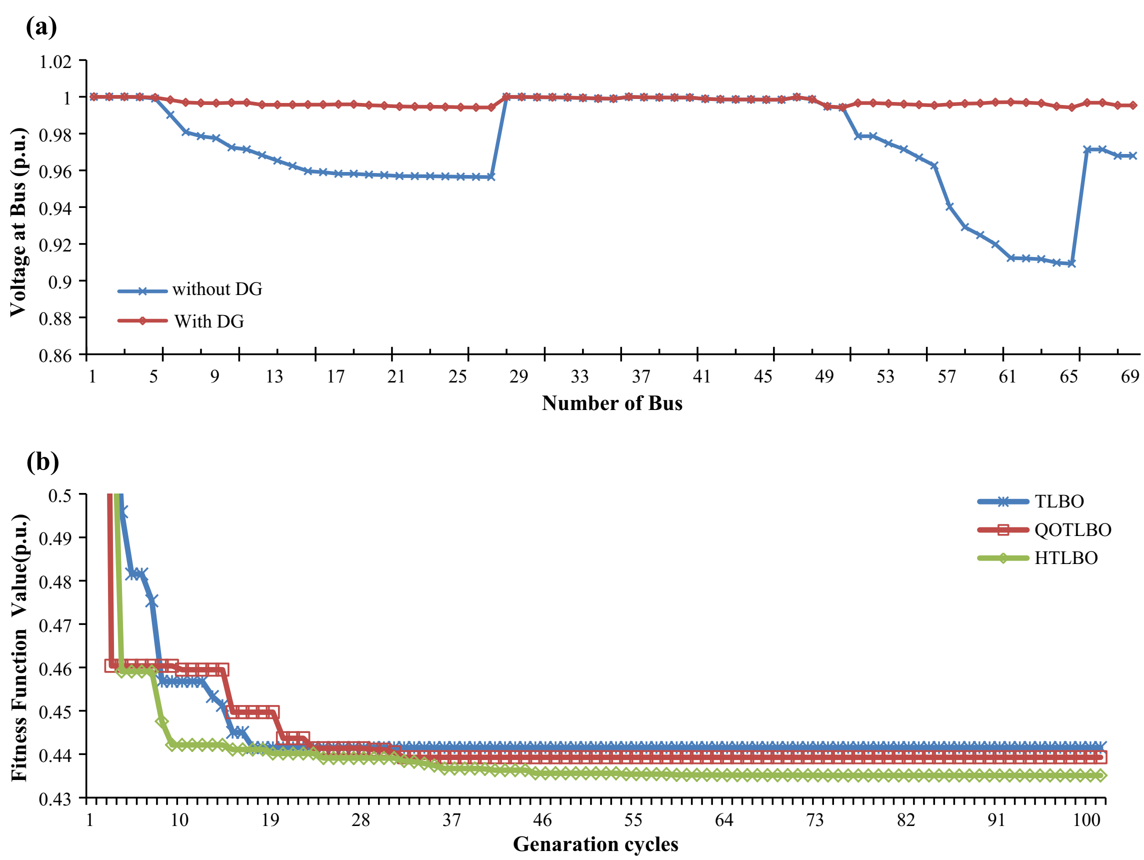

Fig. 5 **a** Voltage distribution of 69-bus radial distribution system with and without DG. **b** Convergence characteristics of 69-bus RDS for multi-objective function for TLBO, QOTLBO and HTLBO

Table 8 Simulation results for MOF using TLBO, QOTLBO and HTLBO of 118-bus RDS

	TLBO (Sultana and Roy 2014)		QOTLBO (Sultana and Roy 2014)		HTLBO		HTLBO	
	Penalty factors (b_1 =1.0, b_2 =0.6, b_3 =0.35)						ε-Constraints method	
	Optimal DG		Optimal DG		Optimal DG		Optimal DG	
	Location	Size (MW)	Location	Size (MW)	Location	Size (MW)	Location	Size (MW)
	35	3.2462	43	1.5880	25	2.0833	22	2.0526
	48	2.8864	49	3.8459	43	1.2457	44	1.1217
	65	2.4307	54	0.9852	52	4.9877	51	4.5526
	72	3.3055	74	3.1904	80	2.6429	77	2.6456
	86	1.9917	80	3.1632	82	34.6417	81	4.6412
	99	1.6040	94	1.9524	93	3.8135	93	3.7620
	111	3.5984	111	3.6013	115	3.2830	115	3.2836
P_{loss} (kW)	705.8980		677.5881		774.946		**658.756**	
VDI (p.u.)	0.0327		0.0233		0.0172		**0.0225**	
VSI^{-1}	1.1699		1.1372		1.1090		**1.0940**	
VSI	0.8548		0.8794		0.9017		**0.8978**	
MOF (p.u.)	0.4361		0.4187		0.4062		–	

Bold indicates the better obtained result

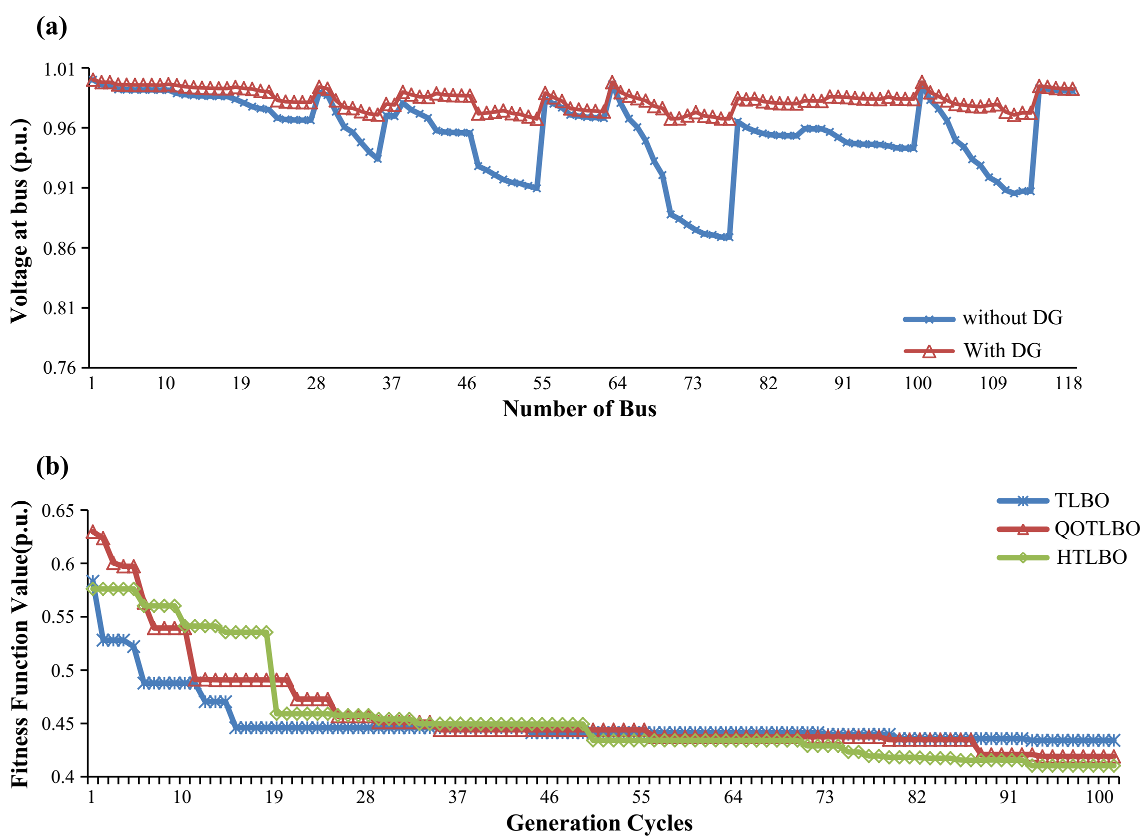

Fig. 6 **a** Voltage distribution of 118-bus radial distribution system with and without DG. **b** Convergence characteristics of 118-bus RDS for multi-objective function for TLBO, QOTLBO and HTLBO

6 Conclusions

A HTLBO technique has been presented in this paper. Its computational capability with continuous variables is first demonstrated on standard mathematical benchmark functions in the form of mean value and standard deviations. Subsequently, the proposed algorithm is implemented for optimal allocation of multiple DGs in the IEEE 33-, 69- and 118-bus RDS to validate their capability with mixed-integer variables (i.e., DGs sizes belong to continuous domain while DG locations are in the discrete domain). The allocation of DGs in RDS is carried out using two methodologies, i.e., weighted sum approach and ε-constraints method, to solve the MOF, which includes the minimization of real power losses and voltage deviations along with maximization of VSI. The ε-constraints approach yields better results than the weighted sum approach in all the objectives over TLBO and QOTLBO. The results authenticate the global convergence competence of the HTLBO. The impact of the various parameters of the proposed algorithm is also investigated. It is observed that for a certain level of DG penetration, a proper tuning of the algorithm parameters ensures global solution. It is also observed that optimal allocation of DGs results in substantial performance improvement of RDS, along with better network congestion management.

Compliance with ethical standards

Conflict of interest The authors declare that they have no conflict of interest.

Ethical approval The article does not contain any studies with human participants or animals performed by any of the authors.

Informed consent Informed consent was obtained from all individual participants included in the study.

Appendix

A MOF optimizes all the SOFs at the same time, subject to the equality and the inequality constraints. In this proposed work, a MOF (Sultana and Roy 2014) simultaneously minimizes F_1 and F_2 along with maximization of F_3.

$$\text{MOF} = \text{Minimize}[b_1 * F_1 + b_2 * F_2 + b_3 * (1/F_3)] \quad \text{(A.1)}$$

If 'm' is total number of objective functions and b_i are penalty coefficients,

$$b_i \in ([0, 1]) \quad \text{and} \quad \sum_{i=1}^{m} b_i = 1$$

If DGs are allocated in RDS with the purpose of meeting a particular objective, the corresponding penalty coefficient value is increased. The priority of objective function in the MOF decides the value of the penalty coefficient. However, the sum of the penalty coefficients must be unity for a normalized objective function.

References

Abu Arqub O (2017) Adaptation of reproducing kernel algorithm for solving fuzzy Fredholm–Volterra integrodifferential equations. Neural Comput Appl 28(7):1591–1610

Abu Arqub O, AL-Smadi M, Momani S (2016) Numerical solutions of fuzzy differential equations using reproducing kernel Hilbert space method. Soft Comput 20:3283–3302

Abu-Mouti FS, El-Hawary ME (2011) Optimal distributed generation allocation and sizing in distribution systems via artificial bee colony algorithm. IEEE Trans Power Deliv 26(4):2090–2101

Ameli A, Bahrami S, Khazaeli F, Haghifam MR (2014) A multiobjective particle swarm optimization for sizing and placement of DGs from DG owners' and distribution company's viewpoints. IEEE Trans Power Deliv 29(4):1831–1840

Arqub OA, Abo-Hammour Z (2014) Numerical solution of systems of second-order boundary value problems using continuous genetic algorithm. Inf Sci 279:396–415

Arqub OA, Al-Smadi M, Momani S (2017) Application of reproducing kernel algorithm for solving second-order, two-point fuzzy boundary value problems. Soft Comput 21:7191–7206

Baran ME, Wu FF (1989) Network reconfiguration in distribution systems for loss reduction and load balancing. IEEE Trans Power Deliv 4(2):1401–1407

Chakravorty M, Das D (2001) Voltage stability analysis of radial distribution networks. Int J Electr Power Energy Syst 23(2):129–135

Chen J, Pan Q, Li J (2012) Harmony search algorithm with dynamic control parameters. Appl Math Comput 219(2):592–604

Das D, Nagi HS, Kothari DP (1994) Novel method for solving radial distribution networks. IEE Proc Gener Transm Distrib 141(4):291–298

Das S, Mukhopadhyay A, Roy A, Abraham A, Panigrahi BK (2011) Exploratory power of the harmony search algorithm: analysis and improvements for global numerical optimization. IEEE Trans Syst Man Cybern Part B (Cybern) 41(1):89–106

Deb K (2001) Multiobjective optimization using evolutionary algorithm, ch. 3. Wiley, Chichester, pp 47–75

Gomez-Gonzalez M, López A, Jurado F (2012) Optimization of distributed generation systems using a new discrete PSO and OPF. Electr Power Syst Res 84(1):174–180

Gopiya Naik SN, Khatod DK, Sharma MP (2015) Analytical approach for optimal siting and sizing of distributed generation in radial distribution networks. IET Gener Transm Distrib 9(3):209–220

Goswami SK, Basu SK (1991) Direct solution of distribution systems. IEE Proc C Gener Transm Distrib 138(1):78–88

Gözel T, Hocaoglu MH (2009) An analytical method for the sizing and siting of distributed generators in radial systems. Electr Power Syst Res 79(6):912–918

Hung DQ, Mithulananthan N, Bansal RC (2010) Analytical expressions for DG allocation in primary distribution networks. IEEE Trans Energy Convers 25(3):814–820

Injeti SK, Prema Kumar N (2013) A novel approach to identify optimal access point and capacity of multiple DGs in a small, medium and large scale radial distribution systems. Int J Electr Power Energy Syst 45(1):142–151

Kanwar N, Gupta N, Niazi KR, Swarnkar A (2015) Simultaneous allocation of distributed resources using improved teaching learning based optimization. Energy Convers Manag 103:387–400

Kanwar N, Gupta N, Niazi KR, Swarnkar A (2017) Optimal allocation of DGs and reconfiguration of radial distribution systems using an intelligent search-based TLBO. Electr Power Compon Syst 45(5):476–490

Kattan A, Abdullah R (2013) Applied Mathematics and Computation A dynamic self-adaptive harmony search algorithm for continuous optimization problems. Appl Math Comput 219(16):8542–8567

Mahdavi M, Fesanghary M, Damangir E (2007) An improved harmony search algorithm for solving optimization problems. Appl Math Comput 188(2):1567–1579

Martín García JA, Gil Mena AJ (2013) Optimal distributed generation location and size using a modified teaching–learning based optimization algorithm. Int J Electr Power Energy Syst 50:65–75

Mohanty B, Tripathy S (2016) A teaching learning based optimization technique for optimal location and size of DG in distribution network. J Electr Syst Inf Technol 3(1):33–44

Moradi MH, Abedini M (2012) A combination of genetic algorithm and particle swarm optimization for optimal DG location and sizing in distribution systems. Int J Electr Power Energy Syst 34(1):66–74

Moravej Z, Akhlaghi A (2013) A novel approach based on cuckoo search for DG allocation in distribution network. Int J Electr Power Energy Syst 44(1):672–679

Nagrath IJ, Kothari DP (2007) Power system engineering, 2nd edn. McGraw Hill Education, New York

Niknam T, Taheri SI, Aghaei J, Tabatabaei S, Nayeripour M (2011) A modified honey bee mating optimization algorithm for multiobjective placement of renewable energy resources. Appl Energy 88(12):4817–4830

Pan Q, Suganthan PN, Tasgetiren MF, Liang JJ (2010) A self-adaptive global best harmony search algorithm for continuous optimization problems. Appl Math Comput 216(3):830–848

Rao RV, Savsani VJ, Vakharia DP (2011) Computer-aided design teaching–learning-based optimization: a novel method for constrained mechanical design optimization problems. Comput Aided Des 43(3):303–315

Saha S, Mukherjee V (2016) Optimal placement and sizing of DGs in RDS using chaos embedded SOS algorithm. IET Gener Transm Distrib 10(14):3671–3680

Sheng W, Liu K, Liu Y, Ye X, He K (2016) Reactive power coordinated optimisation method with renewable distributed generation based on improved harmony search. IET Gener Transm Distrib 10(13):3152–3162

Singh D, Singh D, Verma KS (2008) GA based energy loss minimization approach for optimal sizing & placement of distributed generation. Int J Knowl Based Intell Eng Syst 12(2):147–156

Singh SN, Østergaard J, Jain N (2009) Distributed generation in power systems: an overview and key issues. 24th Indian Engineering Congress, NIT Surathkal, Kerala, 10–13 December 2009

Sultana S, Roy PK (2014) Multi-objective quasi-oppositional teaching learning based optimization for optimal location of distributed generator in radial distribution systems. Int J Electr Power Energy Syst 63:534–545

Teng JH (2003) A direct approach for distribution system load flow solutions. IEEE Trans Power Deliv 18(3):882–887

Tuo S, Zhang J, Yong L, Yuan X, Liu B, Xu X (2015) A harmony search algorithm for high-dimensional multimodal optimization problems. Digit Signal Process 46:151–163

Wang C, Nehrir MH (2004) Analytical approaches for optimal placement of distributed generation sources in power systems. IEEE Trans Power Syst 19(4):2068–2076

Yadav P, Kumar R, Panda SK, Chang CS (2012) An intelligent tuned harmony search algorithm for optimisation. Inf Sci 196:47–72

Zhang D, Fu Z, Zhang L (2007) An improved TS algorithm for loss-minimum reconfiguration in large-scale distribution systems. Electr Power Syst Res 77(5–6):685–694

Zhang Limei, Tang Wei, Liu Yongfu, Lv Tao (2015) Multiobjective optimization and decision-making for DG planning considering benefits between distribution company and DGs owner. Int J Electr Power Energy Syst 73:465–474

Zou D, Gao L, Wu J, Li S (2010) Neurocomputing novel global harmony search algorithm for unconstrained problems. Neurocomputing 73(16–18):3308–3318